Size fractionation and bioavailability of iron released from melting sea ice in the subpolar marginal sea

Naoya Kanna [a, b, c *], Delphine Lannuzel [d], Pier van der Merwe [d], Jun Nishioka [a, c]

[a] Institute of Low Temperature Science, Hokkaido University, Sapporo, Japan

[b] Graduate School of Environmental Earth Science, Hokkaido University, Sapporo, Japan

[c] Arctic Research Center, Hokkaido University, Sapporo, Japan

[d] Institute for Marine and Antarctic Studies, University of Tasmania, Hobart, Australia

[*]Corresponding author at: Arctic Research Center, Hokkaido University, Tel.: +81 11 706 9077.

E-mail address: kanna@arc.hokudai.ac.jp

Keywords: Iron, Sea ice, Bioavailability, Size fraction

Highlights

- Iron released from sea ice was primarily in the particulate form.
- Particulate iron released from sea ice stimulated strong phytoplankton growth.
- The origin of particles in sea ice can be an important factor controlling bioavailability of iron.

Abstract

We incubated Fe-limited seawater with sea-ice sections to evaluate which forms of iron (Fe) released from melting sea ice can favor phytoplankton growth. Biological availability (bioavailability) was approximated by fractionating Fe into soluble (<1,000 kDa), colloidal (1,000 kDa–0.2 μm), and labile particulate (>0.2 μm) sizes. Results show that phytoplankton thrived after the addition of sea ice. While the labile particulate fraction dominated the total Fe pool in sea ice, the concentration of dissolved Fe (<0.2 μm) was likely not enough to support phytoplankton growth in seawater over time. The concentrations and molar ratios of Fe, Mn and Al in acid-digested particles indicate that particulate Fe in sea ice were derived from multiple origins. Specifically, the Fe to Al ratio in sea ice was higher than in lithogenic material, suggesting that the sea ice were enriched with biogenic material. Our study suggests that particulate Fe from sea ice should be considered an important source of biologically available Fe in ice-covered marginal seas.

1. Introduction

The melting of sea ice has recently been recognized as one of the possible processes that supplies iron (Fe) to surface waters, not only in the Antarctic (Grotti et al., 2005; Lannuzel et al., 2007, 2008; van der Merwe et al., 2011a, 2011b; de Jong et al., 2013) but also in the Arctic and sub-Arctic (Aguilar-Islas et al., 2008; Tovar-Sánchez et al., 2010; Kanna et al., 2014; Evans and Nishioka, 2018) regions. Sea-ice meltwaters thus potentially fosters primary production in ice-covered regions in spring.

Previous bioassay experiments have demonstrated that the presence of sea ice in seawater indeed stimulates phytoplankton growth (Sedwick and DiTullio, 1997; Kanna et al., 2018). However, not all Fe in sea ice is available for uptake by phytoplankton. In land-fast ice (sea ice formed in a coastal region and attached to a stationary feature), Fe exists mainly in the particulate form (Grotti et al., 2005; van der Merwe et al., 2011b; de Jong et al., 2013; Lannuzel et al., 2014). However, compared to dissolved Fe (DFe), particulate Fe (PFe) is generally considered less accessible for uptake by phytoplankton (Wells et al., 1995). When sea ice melts, there is a temporal decoupling between the release of DFe and PFe into seawater (van der Merwe et al., 2011a). Dissolved Fe is released first together with sea-ice brines, followed by PFe, which is released later with particulate organic carbon in low-salinity meltwater (Lannuzel et al., 2013).

Dissolved Fe can be further fractionated into soluble and colloidal fractions (e.g., Wu et al., 2001). The size fractionation of DFe into soluble Fe (<100 kDa) and colloidal Fe (100 kDa–0.2 μm) fractions has been investigated by Lannuzel et al. (2014) in Antarctic fast ice. However, there is little information

49 on which size fractions remain in seawater after melting. The origin of the Fe particles found in sea
50 ice is likely to be an important factor controlling Fe bioavailability. Particulate Fe can originate from
51 biogenic, lithogenic and detrital material (Bowie et al., 2010). Previous field studies have partitioned
52 PFe in sea ice into lithogenic (i.e., refractory) and biogenic (i.e., potentially bio-available) fractions to
53 help predict the lability of Fe in sea ice (Lannuzel et al., 2014, 2016a). A previous bioassay experiment
54 suggests that the supply of PFe stored in sea ice allows the growth of phytoplankton in seawater (Kanna
55 and Nishioka, 2016). However, the temporal changes in the concentrations of Fe in the different size
56 fractions released from melting sea ice during phytoplankton growth have not yet been investigated.
57 The detailed physical speciation (i.e., size distribution) of Fe in seawater after the melting of sea ice
58 should therefore be investigated to understand the role of sea ice in supporting phytoplankton growth.
59 In this study, we examined the forms of Fe released from sea ice into seawater and the temporal
60 changes in their concentrations during the growth of phytoplankton. A sea-ice addition incubation
61 experiment was conducted along with the size fractionation of Fe into soluble (<1,000 kDa), colloidal
62 (1,000 kDa–0.2 μm), and labile particulate (>0.2 μm) forms after the release of Fe from sea ice into
63 seawater. The particulate manganese (Mn) and aluminium (Al) in sea ice were also measured to
64 determine whether PFe incorporated into sea ice was derived from biogenic or lithogenic sources. The
65 combined results were used to assess the bioavailability of Fe released from sea ice into seawater.
66
67

2. Materials and methods

2.1 Sample collection and preparation

The sea-ice samples used in this study were collected in the southern Sea of Okhotsk during observational cruises aboard the ice-breaker *Soya* in February 2011 and 2012 (Fig. 1). A full description of the sample collection procedure for trace elements analysis in sea ice is detailed in Kanna et al. (2014). All plastic materials were thoroughly cleaned before use with an alkaline detergent (Merck Millipore), 4 M hydrochloric acid (HCl) or 0.3 M nitric acid (HNO_3) (Wako Pure Chemical Industries) and Milli-Q water (18.2 MΩ Millipore milli-Q system) in a class-100 laminar flow hood in a clean-air laboratory. Field personnel scooped up a block of floating sea ice directly using trace-metal-free PVC gloves, for storage in double plastic bags. The collected sea ice was placed in a freezer (–15 °C) during the cruise before transfer to an onshore cold laboratory (–20 °C). In the cold laboratory, the cleaning process of the sea ice was performed according to previously reported methods (Kanna et al., 2014). The processed sea ice was transferred to high-density-polyethylene (HDPE) or polycarbonate (PC) jars (Thermo Fisher Scientific) and stored at –15 °C until the start of the incubation experiments.

To trace the origin of the PFe incorporated into sea ice, we also prepared particle samples for measuring Fe, Mn and Al. The cleaned and processed sea ice was melted in HDPE or PC jars. The melted sea ice was then filtered through an acid-cleaned 0.2 μm Nucleopore filter (Sterlitech or Whatman) mounted on an acid-cleaned all Teflon or PC filtration apparatus to collect the particles.

87 Filtrates were acidified to pH 1.8 and kept for DFe analysis.

88 We also collected suspended particulate matter (SPM) in seawater in July 2012 in the western
89 subarctic North Pacific during a research cruise of the vessel *Hakuho-maru* (Fig. 1). Approximately
90 304 L of seawater was filtered through an acid-cleaned 1.0 μm Nucleopore filter (Whatman) at a depth
91 of 750 m using a large-volume, in situ filtration system (WTS-6-1-142LV; McLane Research
92 Laboratories). Iron, Mn and Al concentrations in SPM were measured and compared to those in sea
93 ice.

94

95 *2.2 Shipboard incubation experiment*

96 A sea-ice addition incubation experiment was performed in July 2012 during a research cruise
97 onboard *RV Hakuho-Maru* following the method outlined in Kanna and Nishioka (2016). All plastic
98 containers for seawater sampling and the incubation experiment were acid-cleaned in a class-100
99 laminar flow hood in a clean-air laboratory following the method of Takeda and Obata (1995). Surface
100 water and resident biota in the western subarctic North Pacific (Fig. 1) was collected from a depth of
101 20 m using acid-cleaned, Teflon-coated, 12 L Niskin-X samplers attached to a CTD-carousel multi-
102 sampler system. The seawater was transferred into 20 L PC carboys (Thermo Fisher Scientific) and
103 then passed through a 220 μm mesh sieve to eliminate mesozooplankton before dispensing into 500
104 mL PC incubation bottles (Thermo Fisher Scientific). The experiment consisted of duplicate or
105 triplicate incubation bottles for the following treatments: *Control, +$FeCl_3$ treatment* and *+Ice*

106 *treatment*. For the *+$FeCl_3$ treatment*, inorganic $FeCl_3$ (Wako Pure Chemical Industries) was spiked
107 into 500 mL of seawater to achieve a final concentration of 2.5 nM. For the *Ice treatment*, sea ice was
108 melted in an onboard laboratory. 5 mL of a homogenized sea-ice meltwater, which contains
109 macronutrients of 1.1 μM for nitrate and nitrite (NO_3+NO_2), 0.75 μM for phosphate (PO_4) and 1.3 μM
110 for silicate ($Si(OH)_4$), was added to 500 mL of seawater (v:v = 1:100) to mimic the melting of 0.5 m
111 thick sea ice into 50 m of water column. The meltwater that had passed through an acid-cleaned 0.2
112 μm syringe filter (Millex-LG, Merck Millipore) was kept to quantify the initial DFe concentrations in
113 sea ice. The *Control* received no addition of inorganic $FeCl_3$ nor melted sea ice. The PC bottles were
114 incubated for 9 days at 5 °C in an incubator (CN-40A, Mitsubishi Electronic) under a 14 h light:10 h
115 dark cycle with 140 μmol photons m^{-2} s^{-1} of fluorescent light for all treatments. As a result, the light
116 levels remained consistent during the course of the incubation. Duplicate and triplicate incubation
117 bottles from each treatment were used on days 0 and 3 and on days 6 and 9, respectively.

118 At each time step, unfiltered and filtered samples were collected from incubation bottles, after
119 gentle homogenisation. One sub-sample was directly transferred into a 125 mL low-density-
120 polyethylene (LDPE) bottle (Thermo Fisher Scientific) in a class-100 laminar flow hood in the onboard
121 laboratory for total dissolvable Fe (TDFe) (unfiltered). The other sub-sample was size-fractionated
122 inline using a 0.2 μm Durapore filter (Merck Millipore) and a 1,000 kDa hollow fiber Sterapore
123 ultrafilter (Mitsubishi-rayon) according to previously reported trace metal clean ultrafiltration methods
124 (Nishioka and Takeda, 2000; Nishioka et al., 2001). Here, we operationally define soluble Fe (<1,000

kDa), colloidal Fe (1,000 kDa−0.2 μm) and DFe (<0.2 μm, i.e., sum of soluble and colloidal fractions) (Fig. 2). All unfiltered and filtered seawater samples from the incubation experiment were adjusted to pH < 1.8 by adding ultrapure 20% HCl (Tamapure AA-10, Tama Chemicals) and kept at ambient temperature for over a month until analysis. The difference between TDFe and DFe is considered the labile PFe. It should be noted that procedural blanks for soluble Fe and DFe were not determined in this study. However, the lowest concentrations of soluble Fe and DFe in the *Control* bottle were the same concentrations as detection limit (0.05 nM) of our Fe analysis (see section 2.3), indicating that our procedure was suitable for the intended purpose.

Sub-samples for chlorophyll *a* (Chl *a*) and macronutrients analyses were also collected from the incubation bottles. Chlorophyll *a* in samples from the incubated seawaters were filtered sequentially through a 10 μm Nucleopore filter (Whatman) and then through a GF/F filter (Whatman; mean pore-size 0.7 μm) under gentle vacuum (<0.013 MPa) in the onboard laboratory. Chlorophyll *a* on the 10 and 0.7 μm filters was extracted in *N, N*-dimethylformamide (Wako Pure Chemical Industries) for 24 h in the dark at –20 °C (Suzuki and Ishimaru, 1990). For macronutrients, samples were collected from the incubation bottles without filtration, and then stored in 10 mL acrylic tubes at –20 °C for three months until analysis.

2.3. Sample analysis

2.3.1 From the incubation experiment

144 All acidified Fe samples (TDFe, DFe and soluble Fe) were buffered to pH 3.2 with 10 M formic
145 acid-2.4 M ammonium formate buffer (Tamapure AA-10, Tama Chemicals). The concentration of Fe
146 in each buffered sample was determined using a flow injection analytical and chemiluminescence
147 (FIA-CL) system (Kimoto Electric) equipped with an MAF-8HQ (8-quinolinol-immobilized fluoride
148 containing metal alkoxide glass) resin for the pre-concentration and detection of Fe (Obata et al., 1993,
149 1997). The average detection limit was 0.05 nM. Coefficient of variation (CV) is 9% at the 1.1 nM
150 level (n = 10). The DFe concentration in the sea ice used for the incubation experiment was also
151 analyzed using the FIA-CL system described above.
152 Chlorophyll *a* extracted from the GF/F filters was quantified using a Turner Designs model 10-
153 AU fluorometer using the non-acidification method of Welschmeyer (1994). Macronutrient
154 concentrations in the incubated seawaters were determined using an auto-analyzer (QuAAtro, BL TEC
155 Inc.) with a continuous flow system. The macronutrient measurements were calibrated with reference
156 seawater materials (KANSO Technos) for nutrients in seawater. Detection limits for the measurement
157 were determined by the 3σ level of the measurements of low-nutrient-filtered seawater (n = 8), which
158 were 0.03 μM for NO_3+NO_2, 0.08 μM for PO_4, and 0.13 μM for $Si(OH)_4$.
159
160 *2.3.2 Trace metals analysis of particles in sea ice*
161 We used two methods to analyze trace metals particles in sea ice. Particulate Fe, Mn and Al in
162 the sea ice used for the incubation experiment were quantified using an acid digestion-evaporation

163 method similar to Sugiyama (1996). Briefly, particles loaded on the filter were digested in an acid-
164 cleaned 8 mL Teflon vial (Savillex) with the following ultrapure ammonium solution (NH_4OH)
165 (Tamapure AA-100, Tama Chemicals) and acids: HNO_3, perchloric acid ($HClO_4$) and hydrofluoric
166 acid (HF) (Tamapure AA-100, Tama Chemicals). Firstly, 1 mL of 20% NH_4OH was added into the
167 vial to hydrolyze the filter. After standing for 15 h, the mixture was dried on a hot plate at 95 °C. Then,
168 three different acids (0.3 mL of 70% $HClO_4$, 1 mL of 68% HNO_3 and 1 mL of 38% HF) were added
169 into the vial and the particles were digested at 95 °C for 16 h. A mixture of 1 mL of HNO_3 and 0.5 mL
170 of $HClO_4$ was further added to the digest and dry evaporated at 95 °C, and then resuspended in 5 mL
171 of 0.5 M HNO_3. The concentrations of acid-digested PFe, PMn and PAl in solution were determined
172 with a graphite furnace, atomic absorption spectrophotometer (Z-2700, Hitachi High-Tech). The
173 procedure described above was also applied to the SPM filter for the determination of PFe, PMn and
174 PAl concentrations.

175 Particulate trace metals in the sea ice used for the determination of origin of Fe were quantified
176 at the University of Tasmania following the method outlined in Bowie et al. (2010). Briefly, filters
177 retaining particles derived from sea ice were digested in an acid-cleaned 15 mL Teflon vial with a
178 mixture of ultrapure acids (0.5 mL of 32% HCl + 0.25 mL of 67% HNO_3 + 0.25 mL of 47% HF, all
179 Seastar Baseline) at 95°C for 12 h on a Teflon coated hotplate (SCP Science). The digest was dry
180 evaporated at 70°C for 6 h, and the residue was then resuspended in 10 mL of 10% v:v ultrapure HNO_3
181 with 10 ppb indium added as an internal standard. The solutions were analyzed by Sector Field

182 Inductively Coupled Plasma Mass Spectrometry (Finnigan Element II, Thermo Scientific) to
183 determine the levels of acid-digested PFe, PMn and PAl in sea ice. Two different methods were used
184 to quantify PFe, PMn and PAl in sea ice. Blanks and recoveries from both acid digestion treatments
185 were carefully checked by analyzing procedural filter blanks and certified reference materials (Table
186 1). In most cases, sample concentrations were at least 10-fold higher than the blank. Reference
187 materials results indicate that both procedures are suitable for the intended purpose.
188 Filtrates of the sea ice used for the determination of origin of Fe were measured by FIA-CL at the
189 University of Tasmania, using a procedure adapted from de Jong et al. (1998) as described in detail by
190 van der Merwe et al. (2009). This method's detection limit is on average 0.12 nM. The CV for Fe
191 analysis at the 0.28 nM and 0.63 nM Fe levels were 25.8% (n = 8) and 10% (n = 6), respectively. Using
192 this system, the SAFe standard seawater (D2) reference with a consensus value of 0.956 ± 0.024 nM
193 was measured at 0.99 ± 0.05 nM (n = 8)."
194
195 **3. Results**
196 *3.1. Initial concentrations of Chl a and Fe released from sea ice in different size fractions*
197 On day 0 of the sea-ice addition incubation experiment, TDFe concentrations in the *+$FeCl_3$* and
198 *+Ice treatment*s were higher than in the *Control* bottle; moreover, Fe existed in different forms in each
199 treatment (Fig. 2). Dissolved Fe in the *+$FeCl_3$ treatment* accounted for 60% of TDFe. On the other
200 hand, DFe in the *+Ice treatment* accounted for only 3% of TDFe. This result indicates that Fe released

201 from sea ice in seawater is mostly in the particulate form.

202 On day 0 of the sea-ice addition incubation experiment, Chl *a* concentration of small
203 phytoplankton did not differ between the +*Ice treatment* (0.71 μg L^{-1}) and the *Control* (0.70 μg L^{-1})
204 (Fig. 3a). On the other hand, Chl *a* concentration of large phytoplankton was higher in the +*Ice*
205 *treatment* (0.11 μg L^{-1}) compared with the *Control* (0.02 μg L^{-1}) (Fig. 3b). Chlorophyll *a* was not
206 measured directly in the sea-ice meltwater in this study, however, given a 1:100 dilution ratio, the
207 calculated Chl *a* concentration in the sea-ice meltwater was 7.6 μg L^{-1}. Actually, Chl *a* concentration
208 in sea ice from the Sea of Okhotsk often exceeds 10 μg L^{-1} (D. Nomura, personal communications).
209 Considering these indication, large sea-ice algae had been released from sea ice into the +*Ice treatment*.
210

211 *3.2. Evolution of the Fe size fractions, Chl a and macronutrient concentrations during the incubation*
212 *experiment*

213 Figures 3a-b show the changes in Chl *a* concentration of large and small phytoplankton during
214 the incubation. On day 9, Chl *a* concentration of small phytoplankton in the *Control* bottles was not
215 statistically different from that in the +$FeCl_3$ *treatment* (one-way ANOVA; Tukey post-hoc test, $p >$
216 0.2) (Fig. 3a). On the other hand, Chl *a* concentration of large phytoplankton in the *Control* bottles
217 was significantly lower than in the +$FeCl_3$ *treatment* (one-way ANOVA; Tukey post-hoc test, $p < 0.05$)
218 (Fig. 3b), indicating that the growth of large phytoplankton in the *Control* bottles was Fe-limited.
219 Chlorophyll *a* concentration increased between the initial and final days of the incubation in both the

small and large phytoplankton in the *+Ice treatment*. The increases were significantly higher than in the *Control* (one-way ANOVA; Tukey post-hoc tests, $p < 0.05$) (Fig. 3a-b), indicating that the Fe released from the sea ice stimulated the growth of large and small phytoplankton.

The concentrations of the size-fractionated Fe in the *Control* bottles show little change during the course of the incubation (Fig. 4a). On the other hand, DFe concentrations in the *+$FeCl_3$ treatment* decreased significantly (one-way ANOVA; Tukey post-hoc test, $p < 0.005$) during the course of the incubation (Fig. 4b). The soluble Fe concentration decreased from 0.5 ± 0.002 to 0.3 ± 0.04 nM between day 0 and 9 (one-way ANOVA; Tukey post-hoc test, $p < 0.005$). Notably, the colloidal Fe concentration decreased from 1.0 ± 0.1 to 0.4 ± 0.1 nM between day 0 and 9 (one-way ANOVA; Tukey post-hoc test, $p < 0.01$). On the other hand, labile PFe did not differ significantly in the *+$FeCl_3$ treatment* (one-way ANOVA; Tukey post-hoc test, $p > 0.2$). In the *+Ice treatment*, DFe concentrations remained low (0.11 to 0.18 nM) throughout the incubation, while labile PFe did not differ significantly (one-way ANOVA; Tukey post-hoc test, $p > 0.2$) (Fig. 4c). Compared to the *+$FeCl_3$ treatment*, there was little change in the levels of soluble and colloidal Fe during the growth of phytoplankton in the *+Ice treatment*.

In the *Control* bottles, the macronutrient concentrations hardly changed over the 9-day incubation, suggesting little or no biological uptake (Fig. 5). The decrease in macronutrients concentrations in the *+$FeCl_3$* and *+Ice treatments* (Fig. 5) mirror the increase in Chl *a* that occurred during the incubation (Fig. 3). These results demonstrate that the addition of inorganic $FeCl_3$ as well as the Fe released from

239 sea ice, stimulated macronutrient consumption by phytoplankton.

240

241 *3.3. Concentrations of acid-digested PFe, PMn and PAl in sea ice and SPM*

242 The concentrations of PFe, PMn and PAl in the 11 samples of sea ice from the Sea of Okhotsk
243 are presented in Table 2. The results show a high level of heterogeneity between sea-ice samples,
244 ranging from 303 to 14,945 nM for PFe, 3.7 to 255 nM for PMn and 829 to 34,142 nM for PAl. Results
245 also show that the particulate fraction largely dominates (> 99%) the total Fe pool in sea ice from the
246 Sea of Okhotsk (Table 2). For the sample of SPM in seawater, the averaged value of PFe, PMn and
247 PAl (n = 3) was 10,406 ± 1,526 nM for PFe, 24,203 ± 2,895 nM for PMn and 559 ± 74 nM for PAl,
248 respectively.

249

250

251 **4. Discussion**

252 *4.1. Potential availability of labile PFe in sea ice*

253 The results of our incubation experiment reveal that Fe released from sea ice stimulates the growth
254 of phytoplankton (Fig. 3). We cannot rule out a potential bias from the addition of sea-ice algae in the
255 +*Ice treatment*. However, this result is unlikely to be due to seeding of large sea-ice algae alone in the
256 +*Ice treatments.* This is because large algae are unlikely to thrive in Fe-limited conditions experience
257 in the *Control* incubation (Kanna and Nishioka, 2016).

The DFe fraction in the incubation bottles accounted for only 3% of TDFe immediately after the addition of the melted sea ice (day 0, Fig. 2). The initial seawater DFe concentration in the *Control* bottle was 0.05 nM. The initial sea-ice DFe concentration was 8.5 nM. With a 1:100 sea ice:seawater volume ratio, we therefore expect the concentration of DFe to increase to approximately 0.13 nM in the *+Ice treatment* when the sea ice melt-water was added. This is confirmed by DFe concentrations measured on day 0 in the *+Ice treatment* (Fig. 2). The macronutrient concentrations in the *+Ice treatment* were lowered as follows: 0.1 μM for NO_3+NO_2 and PO_4, and 0.04 μM for $Si(OH)_4$ immediately after the addition of the melted sea ice (day 0, Fig. 5). This addition is deemed insignificant as macronutrients were not depleted during any of the incubations (Fig. 5).

To assess whether DFe released from the sea ice is enough to sustain the growth of phytoplankton, we compared the initial DFe concentrations in all treatments with phytoplankton's half saturation constant for Fe (K_{Fe}) reported in the literature. K_{Fe} has been used previously as an indicative limit for Fe limitation (e.g., Blain et al., 2002). The K_{Fe} values for subarctic Pacific phytoplankton range from 0.10 to 0.58 nM for large cells (> 5 μm) and 0.08 to 0.53 nM for small cells (0.7−10 μm) (Noiri et al., 2005; Kudo et al., 2006; Takeda, 2011; Kanna and Nishioka, 2016). Initial DFe in the *Control* bottles (0.05 nM) was close to a lower limit of the reported K_{Fe} values (Fig. 2), suggesting that the low DFe concentrations may limit the growth of large and small phytoplankton in seawater alone. In the *+$FeCl_3$ treatment*, the initial level of DFe (1.5 nM) in the bottles was at least three times greater than an upper limit of the reported K_{Fe} values (Fig. 2), indicating that the level in this treatment is sufficient for the

277 growth of large and small phytoplankton. This is supported by the growth of phytoplankton, especially
278 large cells, in the bottles of the *+$FeCl_3$ treatment* and the absence of growth in the *Control* during the
279 9-day incubation experiment (Fig. 3a-b). The initial level of DFe in the bottles of *+Ice treatment* (0.13
280 nM) was as low as the reported K_{Fe} values (Fig. 2), however, unlike the *Control*, the large and small
281 phytoplankton in the bottles of the *+Ice treatment* thrived during the incubation (Fig. 3a-b). Our result
282 suggests that the labile PFe present in the bottles containing sea ice contributed to the growth of
283 phytoplankton. Due to the relatively low cell surface area to volume ratios, the growth of large
284 phytoplankton is more sensitive to Fe deficiency than that of small phytoplankton (Sunda and
285 Huntsman, 1997; Timmermans et al., 2004). Our results are in agreement with previous laboratory and
286 field studies (e.g., Boyd et al., 1996; Timmermans et al., 2004), showing that the large cells grew faster
287 than the small cells under high Fe conditions.

288 Figure 6 shows the differences in Fe size fractions between the initial and final days of the
289 incubation of the *+$FeCl_3$* and *+Ice treatments*. It should be noted that the differences in the DFe
290 concentrations may be underestimated due to DFe adsorption onto phytoplankton cells. DFe adsorption
291 onto the walls of PC incubation bottles has been shown to be minimal when using the cleaning
292 procedure of Takeda and Obata (1995), as described in detail by Nishioka and Takeda (2000). As
293 phytoplankton grew, DFe concentrations in the *+$FeCl_3$ treatment* decreased to an average
294 concentration of 0.78 nM on day 9 (Fig. 6a). Interestingly, colloidal Fe, which has been recognized as
295 the most dynamic size fraction (e.g., Nishioka and Takeda 2000), decreased significantly between day

296 0 and day 9 (one-way ANOVA; Tukey post-hoc test, $p < 0.001$). The importance of colloidal Fe as a
297 source of bioavailable Fe has been shown in laboratory- and field-based culture studies (Nishioka and
298 Takeda 2000; Nishioka et al., 2003; Chen et al., 2003). In the *+Ice treatment*, labile PFe increased
299 between day 0 and day 9 presumably due to the conversion of refractory PFe into labile fraction of the
300 particulate pools (Fig. 6b). Colloidal Fe concentrations also increased slightly (0.02 nM to 0.07 nM),
301 but not DFe. This result indicates that the *+Ice treatment* contains an exchangeable large particulate
302 pool that may release colloidal and bioavailable Fe in the *+Ice treatment*.
303
304 *4.2. Origin of PFe incorporated into sea ice*
305 Dissolved Fe concentrations were not sufficient to allow the growth of large phytoplankton in the
306 *+Ice treatment*, hence the Fe deficit must have been fulfilled by Fe supplied from the labile particulate
307 fraction. Labile PFe is generally considered less bioavailable than DFe for phytoplankton (Wells et al.,
308 1995). However, bioassay experiments have suggested that PFe in aerosols (Visser et al., 2003), shelf
309 sediments (Hurst and Bruland, 2007; Sugie et al., 2013) and sea ice (Kanna and Nishioka, 2016) are
310 likely available for marine phytoplankton. Notably, biogenic particles (i.e., plankton cell, biogenic
311 detrital material, biogenic opal, carbonate) may be available to phytoplankton through leaching
312 (Ratnarajah et al., 2017), recycling and remineralization (e.g., Landing and Bruland, 1987; Fitzwater
313 et al., 2003) of the particles in seawater (Lam et al., 2015). Here, we discuss molar ratios of PFe and
314 PMn to PAl in sea ice as a proxy to differentiate the biogenic and lithogenic fractions of PFe.

315 Aluminium is often used as an indicator of lithogenic matter because most Al is derived from
316 refractory lithogenic phases. Aluminium is released into seawater from fluvial, aerosol and sediment
317 diagenesis (e.g., Hendry et al., 2010). On the other hand, the bioactive metal Mn is generally used as
318 an indicator of sedimentary redox conditions. Like Fe, Mn is likely to be remobilized via sediment re-
319 suspension (e.g., Froelich et al., 1979). Moreover, the absorption mechanisms and active biological
320 uptake of DFe and DMn in open waters result in the higher level of enrichment of Fe and Mn relative
321 to Al observed in marine particles (Murray and Brewer, 1977). Sea ice is expected to incorporate both
322 lithogenic and biogenic matter during its formation and transport during winter (Lannuzel et al., 2011;
323 de Jong et al., 2013; Kanna et al., 2014). In our study area, sea ice is produced primarily in coastal
324 polynyas on the northwestern continental shelves of the Sea of Okhotsk (Ohshima et al., 2001). Since
325 the continental shelf is a highly productive area (e.g., Saitoh et al., 1996; Sorokin and Sorokin, 1999),
326 higher ratios of Fe and Mn to Al are expected in SPM collected over the shelf (Shigemitsu et al., 2013).
327 Sedimentological evidence suggests that SPM are entrained into newly formed sea ice (Dethleff and
328 Kuhlmann, 2009); this process has been further supported in the Sea of Okhotsk, where winter time
329 turbulent mixing brings SPM over the shelf towards the ocean surface and sea-ice (Ito et al., 2017).
330 Suspended particulate matter with higher ratios of Fe and Mn to Al are therefore expected to be
331 incorporated into sea ice forming in the Sea of Okhotsk.
332 Figure 7 shows the PFe:PAl and PMn:PAl molar ratios in sea ice. Values in subsamples which
333 were split from the sea-ice used in the incubation experiment were presented by white circles in Figure

334 7. For comparison, we show the Fe:Al and Fe:Mn molar ratios in SPM from the western subarctic
335 North Pacific (this study); the Sea of Okhotsk (Shigemitsu et al., 2013), river runoff (Yasuda et al.,
336 2014), Asian mineral dust (Nishikawa et al., 2013; Zhang et al., 2003), aerosols over the Pacific Ocean
337 (Buck et al., 2013) and the upper continental crust (Wedepohl, 1995) in Figure 7. The ratios of Fe and
338 Mn to Al in the upper continental crust, Asian dust and the Pacific Ocean aerosols are indicative of a
339 lithogenic origin. The ratios of PFe:PAl and PFe:PMn in sea ice vary greatly, indicating multiple
340 origins. Some sea ice had higher ratios of PFe and PMn to PAl, suggesting an enrichment in Fe and
341 Mn relative to Al. This could be due to passive absorption onto PFe in sea ice and/or active biological
342 uptake of DFe and DMn by phytoplankton.
343
344 *4.3. Potential processes enhancing bioavailability of Fe released from sea ice*
345 The Fe:Al ratio is a useful proxy to fingerprint the lithogenic or biogenic composition of particles
346 (Lannuzel et al., 2011, 2014, 2016b; Shigemitsu et al., 2013; Ratnarajah et al., 2017), which, in turn,
347 can be used to help predict the lability of Fe particles. For example, high Fe:Al molar ratio near 1 is
348 an indicator for the strong biogenic content of fecal material (Ratnarajah et al., 2017). Our highest
349 PFe:PAl value in sea ice from our incubation experiment (white circles in Fig. 7) is ~1.7, suggesting a
350 large contribution of biogenic materials compared to lithogenic materials. The Fe:Al ratio has been
351 shown to vary between different sea-ice samples (e.g., Fe:Al = ~0.41 in melt ponds of Arctic sea ice
352 [Marsay et al., 2018], ~0.95 in Antarctic land-fast ice [de Jong et al., 2013] and ~2.5 in Antarctic pack

353 ice [van der Merwe et al., 2011; Lannuzel et al., 2011]). Thus, the heterogeneous distributions of PFe
354 in sea ice with a strong biogenic signature would influence the apparent variability of potentially-
355 bioavailable Fe between ice-covered marginal seas. The net bioavailability of Fe released from sea ice
356 is likely determined by the balance between the processes of leaching from PFe and the subsequent
357 rapid utilization of the leached Fe by phytoplankton in seawaters. In this study, there was no apparent
358 increase in DFe in the *+Ice treatment* during the incubation (Fig. 6b), even though labile PFe released
359 from sea ice enhanced phytoplankton growth. Although the specific concentration of Fe leached from
360 the particles was not quantified in this study, a previous study has indicated that Fe is continually
361 leached from biogenic particles such as fecal material (Ratnarajah et al., 2017). Moreover, previous
362 studies have demonstrated that a substantial fraction of PFe may be chemically labile and leachable
363 using 25% acetic acid (Landing and Bruland, 1987; Bruland et al., 2001; Fitzwater et al., 2003). This
364 fraction is thought to include Fe associated with organic phases and carbonate. The origin of the
365 particles incorporated into sea ice is an important factor controlling the bioavailability of Fe in
366 seawaters when sea ice melts.
367
368
369 **5. Conclusion**
370 The results from our study indicate that Fe released from sea ice is derived mostly from the
371 particulate fraction in seawater. A significant fraction (>99%) of the total Fe pool in sea ice resides in

372 the particulate fraction, which is more enriched in biogenic than lithogenic matter. During a 9-day sea-
373 ice addition incubation experiment, the DFe fraction in our sea-ice meltwater treatment accounted for
374 only 3% of the total Fe pool (0.13 nM) after the addition of sea ice melt-water, and the concentrations
375 of Fe in both the soluble and colloidal fractions remained consistent through time. Nevertheless,
376 phytoplankton thrived during this treatment. It is likely that labile PFe derived from sea ice contributed
377 to the growth of phytoplankton. Thus, our results suggest that PFe stored in sea ice can be an important
378 source of biologically available Fe to the ice-covered marginal seas.
379
380 **Acknowledgements**
381 We thank the captain, crew and scientists of the R/V *Hakuho-maru* of the University of Tokyo,
382 and the P/V *Soya* of the Japan Coast Guard for their assistance during the cruise. We wish to thank Ms.
383 A. Murayama for her helpful support with laboratory work. We thank Dr. H. Ogawa for coordinating
384 the R/V *Hakuho-maru*, and Dr. T. Toyota onboard the P/V *Soya* for sea ice sampling. Special thanks
385 to Dr. A. R. Bowie, Dr. K. Suzuki and Mr. C. Dillon for all their efforts to help our efforts. This study
386 was supported by a Grant-in-Aid for Scientific Research (A, B) (No. 17H00775, No.26281002), Grant-
387 in-Aid for Scientific Research in Innovative Areas (No.15H05820) from the Ministry of Education,
388 Culture, Sports, Science and by the Canon Foundation to JN. This research was also supported by
389 Green Network of Excellent Program (GRENE Program), Arctic Climate Change Research Project
390 and the Grant for Joint Research Program of the Institute of Low Temperature Science, Hokkaido

391 University. This work is also supported by funding from Tsuneichi Fujii Scholarship based on an
392 exchange program at the University of Tasmania. Finally, we would like to thank Dr. Thomas Bianchi
393 and two anonymous reviewers for their constructive comments.

394 **References**

395 Aguilar-Islas, A. M., Rember, R. D., Mordy, C. W., Wu, J., 2008. Sea ice-derived dissolved iron and
396 its potential influence on the spring algal bloom in the Bering Sea. Geophys. Res. Lett. 35, L24601.
397 Blain, S., Sedwick, P. N., Griffiths, F. B., Quéguiner, B., Bucciarelli, E., Fiala, M., Pondaven, P.,
398 Tréguer, P., 2002. Quantification of algal iron requirements in the Subantarctic Southern Ocean
399 (Indian sector). Deep-Sea Res. II 49 (16), 3255–3273.
400 Bowie, A. R., Townsend, A. T., Lannuzel, D, Remenyi, T. A., van der Merwe, P., 2010. Modern
401 sampling and analytical methods for the determination of trace elements in marine particulate
402 material using magnetic sector inductively coupled plasma–mass spectrometry. Anal. Chim. Acta
403 676, 15-27.
404 Boyd, P. W., Muggli, D. L., Varela, D. E., Goldblatt, R. H., Chretien, R., Orians, K. J., Harrison, P. J.,
405 1996. In vitro iron enrichment experiments in the NE subarctic Pacific. Mar. Ecol. Prog. Ser. 136,
406 179–193.
407 Bruland, K. W., Rue, E. L., Smith, G. J., 2001. Iron and macronutrients in California coastal upwelling
408 regimes: Implications for diatom blooms. Limnol. Oceanogr. 46 (7), 1661–1167.
409 Buck, C. S., Landing, W. M., Resing, J., 2013. Pacific Ocean aerosols: Deposition and solubility of
410 iron, aluminum, and other trace elements. Mar. Chem., 157, 117-130.
411 Chen, M., Dei, R. C. H., Wang, W-X., Guo, L., 2003. Marine diatom uptake of iron bound with natural
412 colloids of different origins. Mar. Chem. 81, 177-189.

de Jong, J. T. M., den Das, J., Bathmann, U., Stoll, M. H. C., Kattner, G., Nolting, R. F., de Baar, H. J. W., 1998. Dissolved iron at subnanomolar levels in the Southern Ocean as determined by ship-board analysis. Anal. Chim. Acta 377, 113-124.

de Jong, J. T. M., Schoemann, V., Maricq, N., Mattielli, N., Langhorne, P., Haskell, T., Tison, J-L., 2013. Iron in land-fast sea ice of McMurdo Sound derived from sediment resuspension and wind-blown dust attributes to primary productivity in the Ross Sea, Antarctica. Mar. Chem. 157, 24–40.

Dethleff, D., Kuhlmann, G., 2009. Entrainment of fine-grained surface deposits into new ice in the southwestern Kara Sea, Siberian Arctic. Cont. Shelf Res. 29 (4), 691–701.

Evans, L. K., Nishioka, J., 2018. Quantitative analysis of Fe, Mn and Cd from sea ice and seawater in the Chukchi Sea, Arctic Ocean. Polar Science 17, 50-58.

Fitzwater, S. E., Johnson, K. S., Elrod, V. A., Ryan, J. P., Coletti, L. J., Tanner, S. J., Gordon, R. M., Chavez, F. P., 2003. Iron, nutrient and phytoplankton biomass relationships in upwelled waters of the California coastal system. Cont. Shelf Res. 23, 1523–1544.

Froelich, P.N., et al., 1979. Early oxidation of organicmatter in pelagic sediments of the eastern equatorial Atlantic: suboxic diagenesis. Geochim Cosmochim. Acta 43, 1075–1090.

Grotti, M., Soggia, F., Ianni, C., Frache, R., 2005. Trace metals distributions in coastal sea ice of Terra Nova Bay, Ross Sea, Antarctica. Antarct. Sci. 17, 289–300.

Hendry, K.R., Meredith, M.P., Measures, C.I., Carson, D.S., Rickaby, R.E.M., 2010. The role of sea

ice formation in cycling of aluminium in northern Marguerite Bay, Antarctica. Estuarine, Coastal and Shelf Sci. 87, 103–112.

Hurst, M., Aguilar-Islas, A. M., Bruland, K. W., 2010. Iron in the southeastern Bering Sea: elevated leachable particulate Fe in shelf bottom waters as an important source for surface waters. Cont. Shelf Res. 30, 467–480.

Ito, M., K. I. Ohshima, Y. Fukamachi, G. Mizuta, Y. Kusumoto, and J. Nishioka (2017), Observations of frazil ice formation and upward sediment transport in the Sea of Okhotsk: A possible mechanism of iron supply to sea ice, J. Geophys. Res. Oceans, 122, 788–802, doi:10.1002/2016JC012198.

Kanna, N., Nishioka, J., 2016. Bio-availability of iron derived from subarctic first-year sea ice. Mar. Chem. 186, 189-197.

Kanna, N., Toyota, T., Nishioka, J., 2014. Iron and macro-nutrient concentrations in sea ice and their impact on the nutritional status of surface waters in the southern Okhotsk Sea. Prog. Oceanogr. 126, 44–57.

Kanna, N., Sibano, Y., Toyota, T., Nishioka, J., 2018. Winter iron supply processes fueling spring phytoplankton growth in a sub-polar marginal sea, the Sea of Okhotsk: Importance of sea ice and the East Sakhalin Current. Mar. Chem. 206, 109-120.

Kudo, I., Noiri, Y., Nishioka, J., Taira, Y., Kiyosawa, H., Tsuda, A., 2006. Phytoplankton community response to Fe and temperature gradients in the NE (SERIES) and NW (SEEDS) subarctic Pacific

451 Ocean. Deep Sea Res. II 53, 2201-2213.
452 Lam, P.J., Twining, B.S., Jeandel, C., Roychoudhury, A.N., Resing, J.A., Santschi, P.H., Anderson,
453 R.F., 2015. Methods for analyzing the concentration and speciation of major and trace elements
454 in marine particles. Prog. Oceanogr. 133, 1–26.
455 Landing, W. M., Bruland, K. W., 1987. The contrasting biogeochemistry of iron and manganese in the
456 Pacific Ocean. Geochim. Cosmochim. Acta 51 (1), 29–43.
457 Lannuzel, D., Schoemann, V., de Jong, J., Tison, J-L., Chou, L., 2007. Distribution and
458 biogeochemical behavior of iron in the East Antarctic sea ice. Mar. Chem. 106 (1-2), 18-32.
459 Lannuzel, D., Schoemann, V., de. Jong, J., Chou, L., Delille, B., Becquevort, S., Tison, J-L., 2008.
460 Iron study during a time series in the western Weddell pack ice. Mar. Chem. 108, 85–95.
461 Lannuzel, D., Schoemann, V., Dumont, I., Content, M., de Jong, J., Tison, J-L., Delille, B., Becquevort,
462 S., 2013. Effect of melting Antarctic sea ice on the fate of microbial communities studied in
463 microcosms. Polar Biol. 36, 1483–1497.
464 Lannuzel, D., Bowie, A. R., van der Merwe, P. C., Townsend, A. T. Schoemann, V., 2011, Distribution
465 of dissolved and particulate metals in Antarctic sea ice. Mar. Chem. 124, 134-146.
466 Lannuzel, D., van der Merwe, P., Townsend, A. T., Bowie, A. R., 2014. Size fractionation of iron,
467 manganese and aluminium in Antarctic fast ice reveals a lithogenic origin and low iron solubility.
468 Mar. Chem. 161, 47–56.
469 Lannuzel, D., Chever, F., van der Merwe, P., Janssens, J., Roukaerts, A., Cavagna, A-J., Townsend,

A. T., Bowie, A. R. Meiners, K. M., 2016a. Iron biogeochemistry in Antarctic pack ice during SIPEX-2. Deep Sea Res-II. 131, 111-122.

Lannuzel, D., Vancoppenolle, M., van der Merwe, P., de Jong, J., Meiners, K.M., Grotti, M., Nishioka, J., Schoemann, V., 2016b. Iron in sea ice: Review and new insights. Elem Sci Anth 4, p.000130.

Marsay, C. M., Aguilar-Islas, A., Fitzsimmons, J. N., Hatta, M., Jensen, L. T., John, S. G., Kadko, D., Landing, W. M., Lanning, N. T., Morton, P. L., Pasqualini, A., Rauschenberg, S., Sherrell, R. M., Shiller, A. M., Twining, B. S., Whitmore, L. M., Zhang, R., Buck, C. S., 2018, Dissolved and particulate trace elements in late summer Arctic melt ponds. Mar. Chem. 204, 70-85.

Murray, J.W., Brewer, P.G., 1977. The mechanisms of removal of iron, manganese and other trace metals from seawater. In: Glasby, G.P. (Ed.), Marine Manganese Deposits. Elsevier, Holland, pp. 291–325.

Nishikawa, M., Batdorj, D., Ukachi, M., Onishi, K., Nagano, K., Mori, I., Matsui, I., Sano, T., 2013. Preparation and chemical characterisation of an Asian mineral dust certified reference material. Analytical Methods 5, 4088-4095.

Nishioka, J., Takeda, S., 2000. Change in the concentrations of iron in different size fractions during growth of the oceanic diatom Chaetoceros sp.: importance of small colloidal iron. Mar. Biol. 137, 231-238.

Nishioka, J., Takeda, S., Kudo, I., Tsumune, D., Yoshimura, T., Kuma, K., Tsuda, A., 2003. Size-fractionated iron distributions and iron-limitation processes in the subarctic NW Pacific. Geophys.

Res. Lett. 30.

Nishioka, J., Takeda, S., Wong, C. S., Johnson, W. K., 2001. Size-fractionated iron concentrations in the northeast Pacific Ocean: distribution of soluble and small colloidal iron. Mar. Chem. 74, 157-179.

Noiri, Y., Kudo, I., Kiyosawa, H., Nishioka, J., Tsuda, A., 2005. Influence of iron and temperature on growth, nutrient utilization ratios and phytoplankton species composition in the western subarctic Pacific Ocean during the SEEDS experiment. Prog. Oceanogr. 64, 149-166.

Obata, H., Karatani, H., Nakayama, E., 1993. Automated determination of iron in seawater by chelating resin concentration and chemiluminescence detection. Anal. Chem. 65, 1524–1528.

Obata, H., Karatani, H., Matsui, M., Nakayama, E., 1997. Fundamental studies for chemical speciation of iron in seawater with an improved analytical method. Mar. chem. 56, 97–106.

Ohshima, K. I., Mizuta, G., Itoh, M., Fukamachi, Y., Watanabe, T., Nabae, Y., Suehiro, K., Wakatsuchi, M., 2001. Winter Oceanographic Conditions in the Southwestern Part of the Okhotsk Sea and Their Relation to Sea Ice. J. Oceanogr. 57, 451–460.

Ratnarajah, L., Lannuzel, D., Townsend, A. T., Meiners, K. M., Nicol, S., Friedlaender, A. S., Bowie, A. R., 2017. Physical speciation and solubility of iron from baleen whale fecal material. Mar. Chem. 194, 79-88.

Saitoh, S., Kishino, M., Kiyofuji, H., Taguchi, S., Takahashi, M., 1996. Seasonal variability of phytoplankton pigment concentration in the Okhotsk Sea. J. Remote Sens. Soc. Japan 16, 172–

178.

Sedwick, P. N. and DiTullio, G. R., 1997. Regulation of algal blooms in Antarctic Shelf Waters by the release of iron from melting sea ice. Geophys. Res. Lett. 24, 2515-2518.

Shigemitsu, M., Nishioka, J., Watanabe, Y. W., Yamanaka, Y., Nakatsuka, T., Volkov, Y. N., 2013. Fe/Al ratios of suspended particulate matter from intermediate water in the Okhotsk Sea: Implications for long-distance lateral transport of particulate Fe. Mar. Chem. 157, 41-48.

Sorokin, Y.I., Sorokin, P.Y., 1999. Production in the Sea of Okhotsk. J. Plankton Res. 21, 201–230.

Sugie, K., Nishioka, J., Kuma, K., Volkov, Y. N., Nakatsuka T., 2013. Availability of particulate Fe to phytoplankton in the Sea of Okhotsk. Mar. Chem. 152, 20–31.

Sugiyama, M., 1996. Simultaneous multi-element analysis of aquatic suspended particulate matter. Bunseki Kagaku (in Japanese) 45, 667–675.

Sunda, W. G., S. A. Huntsman, 1997. Interrelated influence of iron, light and cell size on marine phytoplankton growth. *Nature* 390, 389-392.

Suzuki, R., Ishimaru, T., 1990. An improved method for the determination of phytoplankton chlorophyll using N,N-dimethylformamide. J. Oceanogr. 46, 190–194.

Takeda, S., 2011. Iron and phytoplankton growth in the subarctic North Pacific. Aqua-Biosci. Monogr. 4, 41–93.

Takeda, S., Obata, H., 1995. Response of equatorial Pacific phytoplankton to subnanomolar Fe enrichment. Mar. Chem. 50, 219–227.

527 Timmermans, Klaas R., van der Wagt, Bas, de Baar, Hein J. W., 2004. Growth rates, half-saturation
528 constants, and silicate, nitrate, and phosphate depletion in relation to iron availability of four large,
529 open-ocean diatoms from the Southern Ocean. Limnol. Oceanogr. 6, doi:
530 10.4319/lo.2004.49.6.2141.
531 Tovar-Sánchez, A., Duarte, C. M., Alonso, J. C., Lacorte, S., Tauler, R., Galbán-Malagón, C., 2010.
532 Impacts of materials and nutrients released from melting multiyear Arctic sea ice. J. Geophys. Res.
533 115, C07003, http://dx.doi.org/10.1029/2009JC005685.
534 van der Merwe, P., Lannuzel, D., Mancuso Nichols, C. A., Meiners, K., Heil, P., Norman, L., Thomas,
535 D. N., Bowie, A. R., 2009. Biogeochemical observations during the winter–spring transition in
536 East Antarctic sea ice: Evidence of iron and exopolysaccharide controls. Mar. Chem. 115, 163-
537 175.
538 van der Merwe, P., Lannuzel, D., Bowie, A. R., Mancuso Nichols, C. A., Meiners K., 2011a. Iron
539 fractionation in pack and fast ice in East Antarctica: Temporal decoupling between the release of
540 dissolved and particulate iron during spring melt. Deep-Sea Res. II 58, 1222–1236.
541 van der Merwe, P., Lannuzel, D., Bowie, A. R., Meiners K. M., 2011b. High temporal resolution
542 observations of spring fast ice melt and seawater iron enrichment in East Antarctica. J. Geophys.
543 Res. 116, G03017, http://dx.doi.org/10.1029/2010JG001628.
544 Visser, F., Gerringa, L. J. A., Van der gaast, S. J., De Baar, H. J. W., Timmermans, K. R., 2003. The
545 role of the reactivity and content of iron of aerosol dust on growth rates of two Antarctic diatom

546 species. J. Phycol. 39, 1085–1094.

547 Wedepohl, H.K., 1995. The composition of the continental crust. Geochim Cosmochim. Acta 59,

548 1217–1232.

549 Wells, M. L., Price, N. M., Bruland, K. W., 1995. Iron chemistry in seawater and its relationship to

550 phytoplankton: a workshop report. Mar. Chem. 48, 157–182.

551 Welshmeyer, N. A., 1994. Fluorometric analysis of chlorophyll *a* in the presence chlorophyll *b* and

552 phaeopigments. Limnol. Oceanogr. 39, 1985–1992.

553 Wu, J., Boyle, E., Sunda, W., Wen, L-S., 2001. Soluble and Colloidal Iron in the Oligotrophic North

554 Atlantic and North Pacific. Science 293, 847-849.

555 Yasuda, T., Asahara, Y., Ichikawa, R., Nakatsuka, T., Minami, H., Nagao, S., 2014. Distribution and

556 transport processes of lithogenic material from the Amur River revealed by the Sr and Nd isotope

557 ratios of sediments from the Sea of Okhotsk. Prog. Oceanogr. 126, 155-167.

558 Zhang, X. Y., Gong, S. L., Arimoto, R., Shen, Z. X., Mei, F. M., Wang, D., Cheng, Y., 2003.

559 Characterization and Temporal Variation of Asian Dust Aerosol from a Site in the Northern

560 Chinese Deserts. J. Atmos. Chem., 44, 241-257.

Table captions

Table 1 Measurements of filter blanks and the following certified reference materials: granodiorite JG1a and lake sediment JLk-1 (provided by National Institute of Advanced Industrial Science and Technology, Japan), marine plankton BCR-414 (provided by Institute for Reference Materials and Measurements, Belgium) and marine sediment MESS-3 (provided by National Research Council, Canada). Values in parentheses represent uncertified but indicative values. Al is only indicative value in BCR-414, not certified. i. e., the techniques used to analyse Al in BCR-414 probably underestimate Al content.

Table 2 Concentrations of DFe and acid-digested PFe, PAl and PMn in sea ice collected in the Sea of Okhotsk. Sea ice samples collected in 2011 were used in the incubation experiment. Dissolved Fe concentration in sea-ice meltwater which was added to incubation bottles of +*Ice treatment* during incubation experiment is represented by the asterisk. The DFe, PFe, PAl and PMn in sea ice samples collected in 2012 were analyzed at the University of Tasmania.

Figure captions

Fig. 1 Sampling locations of incubation seawater and marine suspended particulate matter (SPM) (●), and sea ice (△ for 2011 cruise; □ for 2012 cruise) used in this study. Sampling locations of both seafloor surface sediment and SPM (◊) are cited from Shigemitsu et al. (2013) and Yasuda et al. (2014).

Fig. 2 Size-fractionated Fe concentrations in incubation bottles of *Control*, *+$FeCl_3$ treatment* and *+Ice treatment* on the initial day of the incubation experiment. The inset shows the definition of the size-fractionated Fe as soluble (<1000 kDa), colloidal (1000 kDa–0.2 μm) and labile particulate [the difference between TDFe (unfiltered) and DFe (<0.2 μm, i.e., sum of soluble Fe and colloidal Fe)] fractions.

Fig. 3 Changes in (a) small-sized and (b) large-sized Chl *a* concentrations in incubation bottles of *Control*, *+$FeCl_3$ treatment* and *+Ice treatment* during the incubation experiment. Values are the means, and error bars are the standard deviations of duplicate or triplicate bottles for each treatment.

Fig. 4 Changes in size-fractionated Fe concentrations in the bottles of (a) *Control*, (b) *+$FeCl_3$ treatment* and (c) *+Ice treatment*. Values are the means, and error bars are the standard deviations of duplicate or triplicate bottles for each treatment.

Fig. 5 Changes in (a) NO_3+NO_2, (b) PO_4 and (c) $Si(OH)_4$ concentrations in incubation bottles of *Control*, *+$FeCl_3$ treatment* and *+Ice treatment* during the incubation experiment. An outlier for *Control* on day 3 is shown in parentheses. This data point was removed from the discussion. Values are the means, and error bars are the standard deviations of duplicate or triplicate bottles for each treatment.

Fig. 6 The size-fractionated Fe concentration shown as the difference between the final and initial days of the incubations of (a) *+$FeCl_3$ treatment* and (b) *+Ice treatment*. Values are the means, and error bars are the standard deviations.

Fig. 7 Plot of acid-digested particulate Fe:Al versus Mn:Al in sea ice and the north Pacific suspended particulate matter (NP-SPM) determined in this study. The value for the subsample of the sea ice used in the incubation experiment is represented by the asterisk in the graph legend. The values corresponding to particles from other external sources (See Fig. 1 for sampling location): SPM (Okh basin-SPM and Okh shelf-SPM) and seafloor surface sediment (Okh shelf-sediment) from the Sea of Okhotsk, and SPM from Amur River (River-SPM) (Shigemitsu et al., 2013; Yasuda et al., 2014). Values of continental crust (Wedepohl, 1995), Asian mineral dust (Asian-dust A and B) (Nishikawa et al., 2013; Zhang et al., 2003) and the Pacific Ocean aerosols (Buck et al., 2013) are indicated by the cross mark and triangles, respectively.

Table 1

	Elements		
	PFe	**PAl**	**PMn**
Method: Sugiyama (1996)			
Procedural filter blank (μg L^{-1})			
Measured (n = 19)	1.8 ± 1	0.3 ± 0.3	0.01 ± 0.01
JG1-a (Fe, Al %; Mn mg kg^{-1})			
*Certified	1.40 ± 0.05	7.57 ± 0.1	454 ± 33
Measured (n = 10)	1.25 ± 0.08	7.27 ± 0.58	438 ± 89
Recovery (%)	89	97	97
JLk-1 (Fe, Al %; Mn mg kg^{-1})			
*Certified	4.85	8.85	2050
Measured (n = 10)	4.80 ± 0.18	8.82 ± 0.73	2285 ± 151
Recovery (%)	99	99	111
Method: Bowie et al. (2010)			
Procedural filter blank (μg L^{-1})			
Measured (n = 3)	1.7 ± 2	1.5 ± 1	0.01 ± 0.01
BCR-414 (mg kg^{-1})			
*Certified [indicative]	[1850 ± 190]	[1800 ± 30]	299 ± 13
Measured (n = 2)	1841 ± 205	2653 ± 292	263 ± 24
Recovery (%)	100	147	88
MESS-3 (mg kg^{-1})			
*Certified	43400 ± 1100	85900 ± 2300	324 ± 12
Measured (n = 2)	42238 ± 1548	75324 ± 7723	315 ± 15
Recovery (%)	97	88	97

Table 2

Sampling date	Elements (nM)				Analytical methods used in this study
	DFe	PFe	PAl	PMn	
16 Feb. 2011	1.7	2371	1436	37	DFe: Obata et al. (1993, 1997)
	6.1	4571	3226	76	Acid-digested PFe, PAl, PMn: Sugiyama (1996)
	5.3	14945	34142	255	
	8.5*	N.D	N.D	N.D	
13 Feb. 2012	0.7	468	1802	16	DFe: de Jong et al. (1998)
	0.6	303	829	11	Acid-digested PFe, PAl, PMn: Bowie et al. (2010)
	N.D	432	1242	16	
	N.D	779	2877	20	
14 Feb. 2012	3.2	858	2969	27	
	3.4	1125	1831	32	
	2.5	359	1311	3.7	
	3.6	782	2640	4.9	

Figure 1

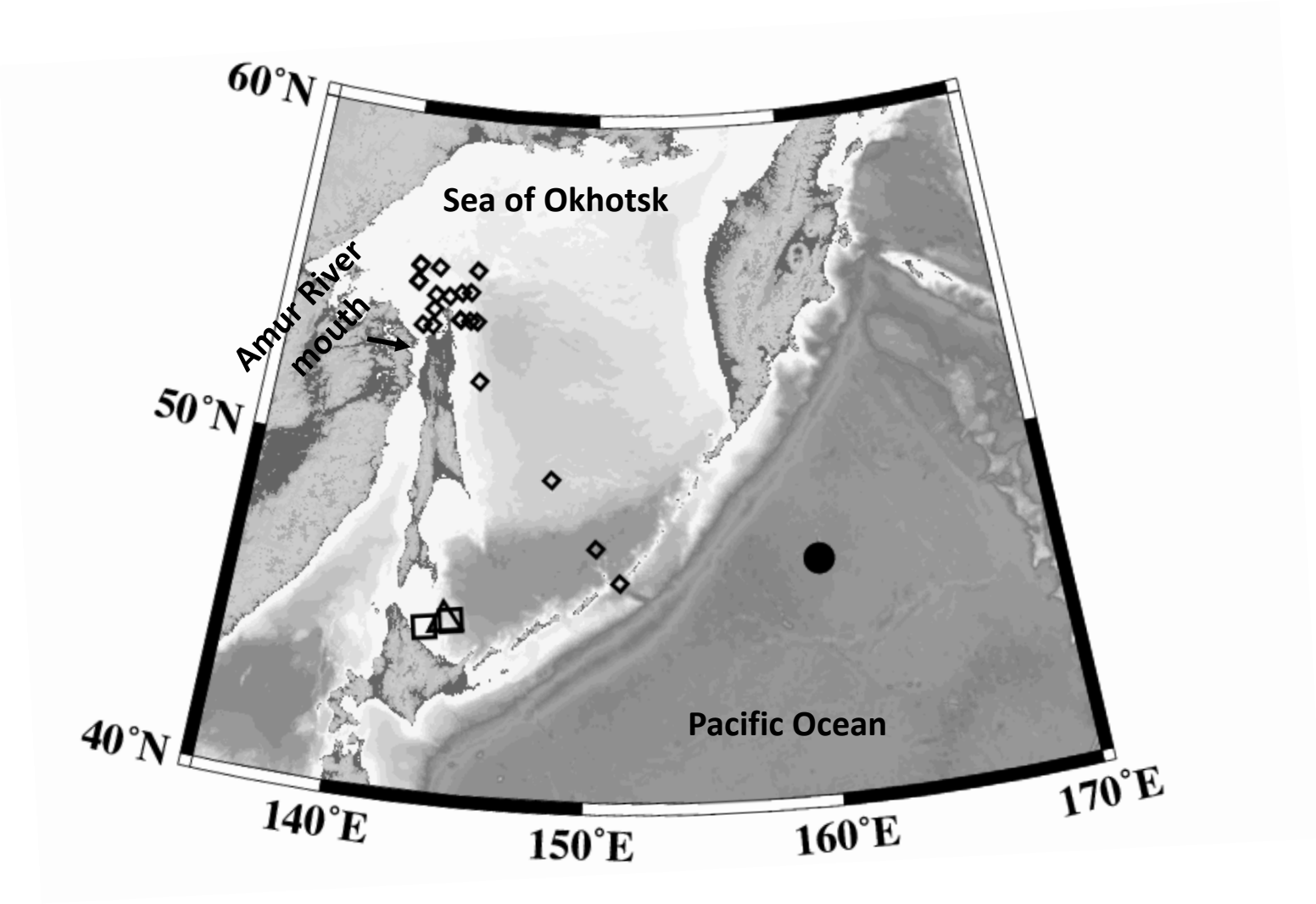
60°N
50°N
40°N
140°E
150°E
160°E
170°E
Sea of Okhotsk
Amur River mouth
Pacific Ocean

Figure 2

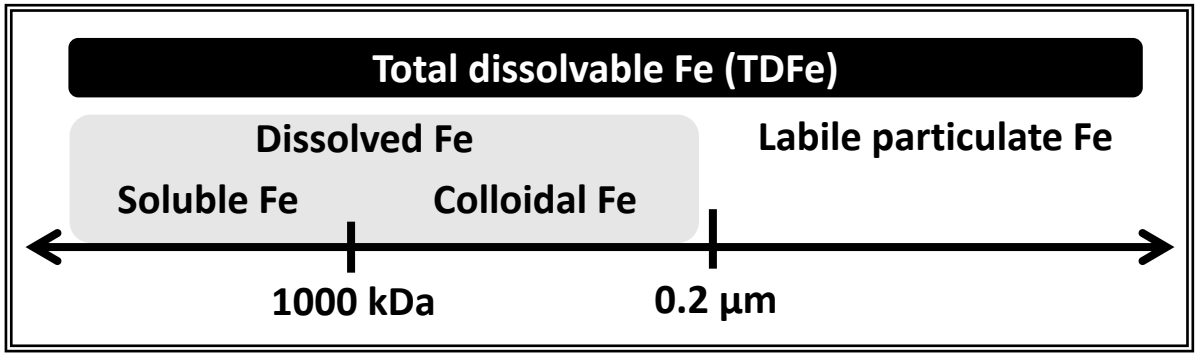
Total dissolvable Fe (TDFe)
Dissolved Fe
Soluble Fe
Colloidal Fe
Labile particulate Fe
1000 kDa
0.2 µm

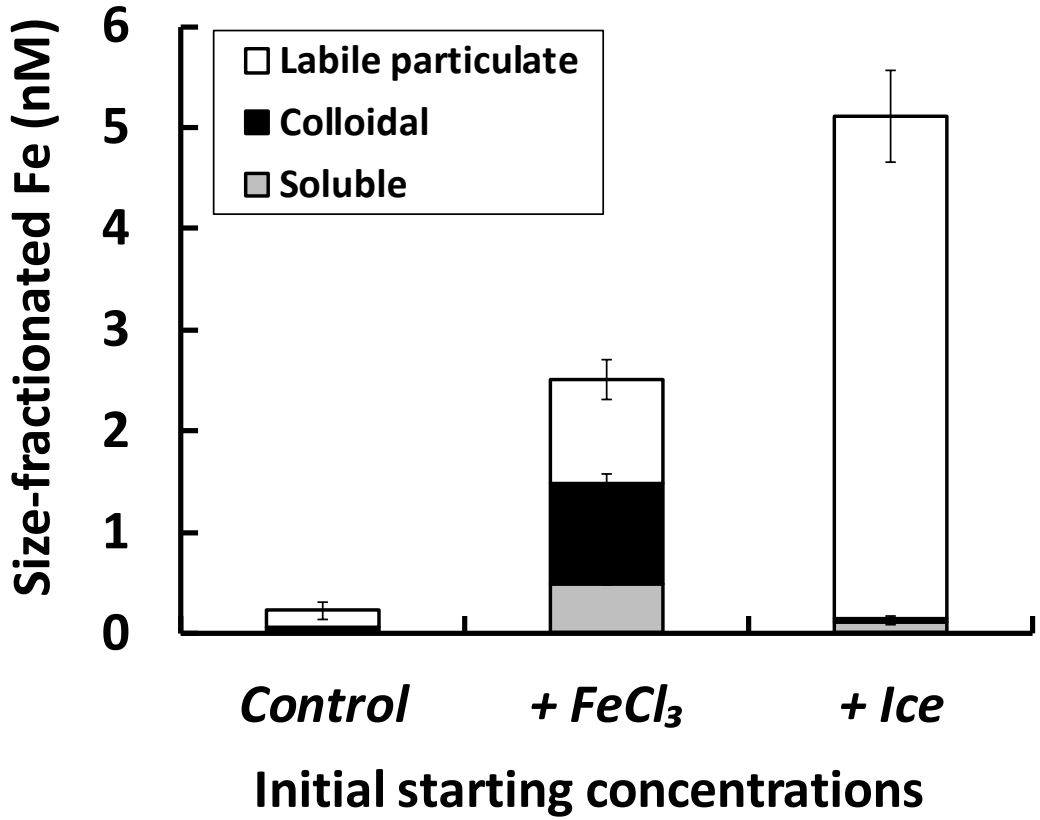
Size-fractionated Fe (nM)
6
5
4
3
2
1
0
Labile particulate
Colloidal
Soluble
Control
+ FeCl₃
+ Ice
Initial starting concentrations

Figure 3

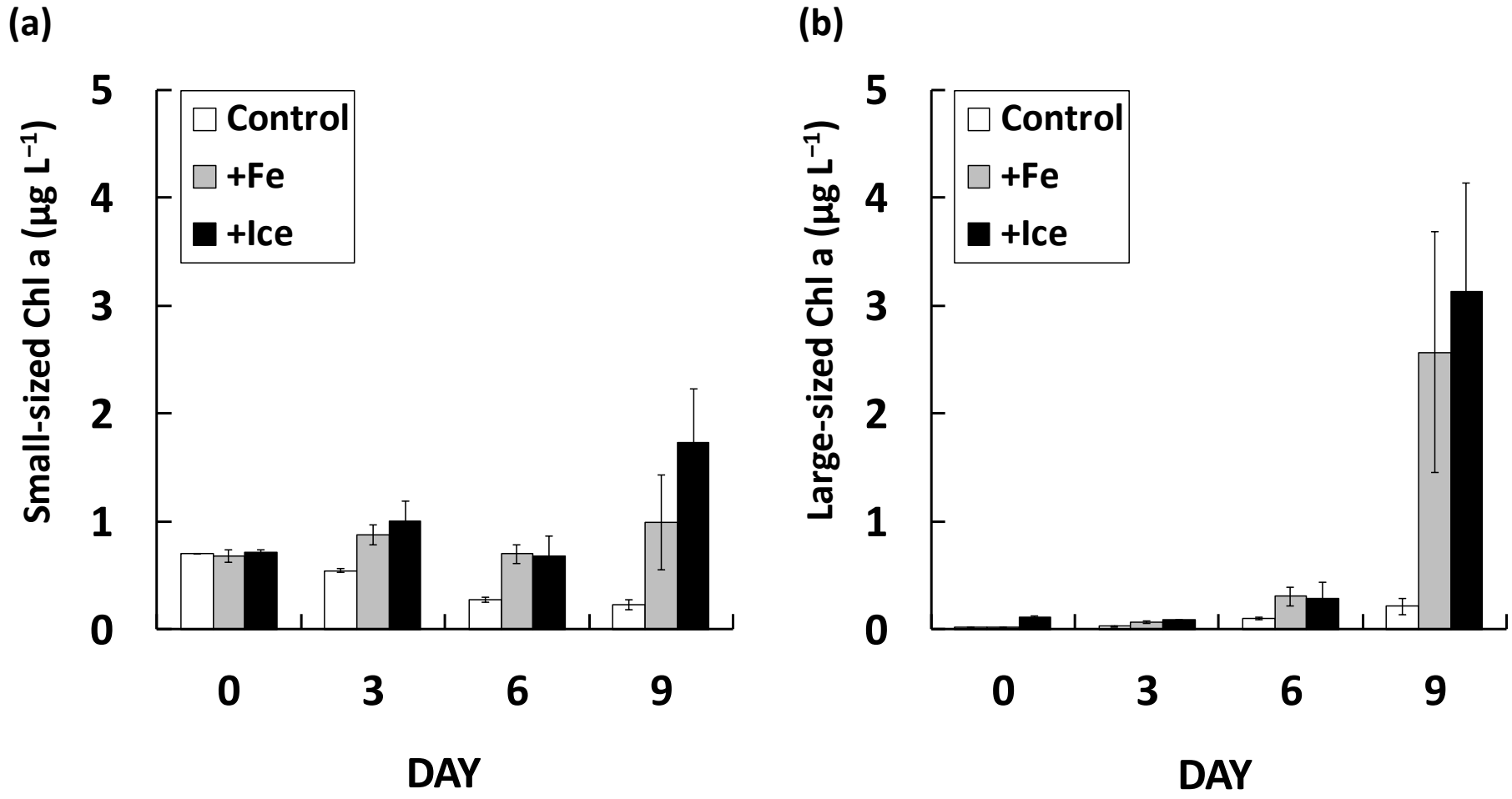
(a)
Small-sized Chl a (μg L⁻¹)
Control
+Fe
+Ice
0
1
2
3
4
5
0
3
6
9
DAY
(b)
Large-sized Chl a (μg L⁻¹)
Control
+Fe
+Ice
0
1
2
3
4
5
0
3
6
9
DAY

Figure 4

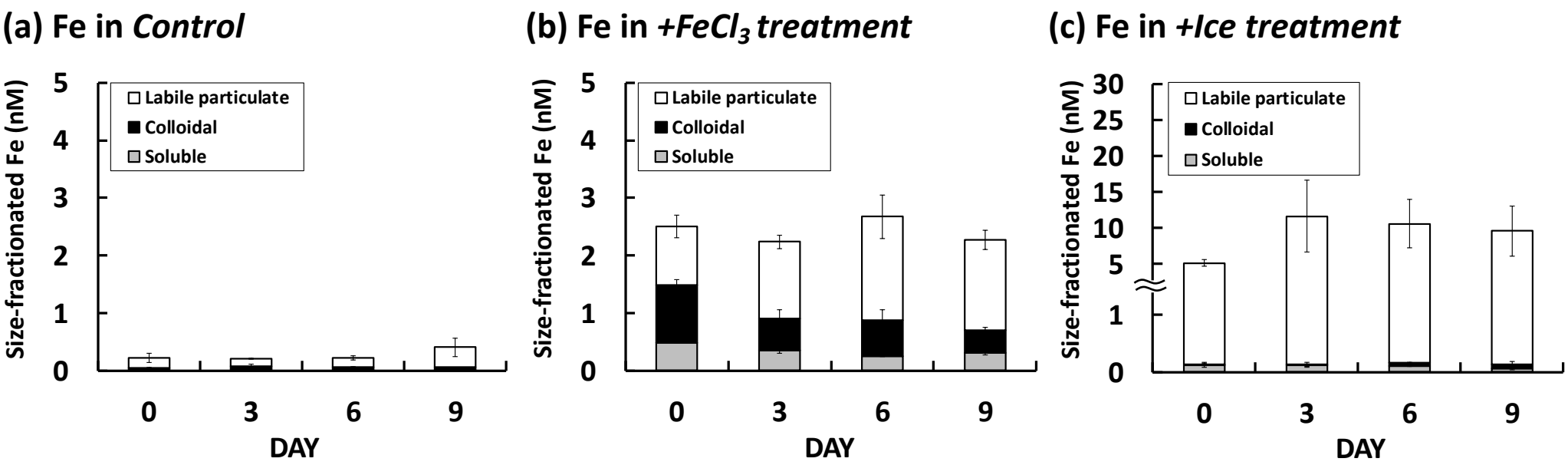
(a) Fe in *Control*
(b) Fe in *+FeCl$_3$ treatment*
(c) Fe in *+Ice treatment*
Size-fractionated Fe (nM)
Labile particulate
Colloidal
Soluble
DAY
0
3
6
9
0
1
2
3
4
5
0
1
5
10
15
20
25
30

Figure 5

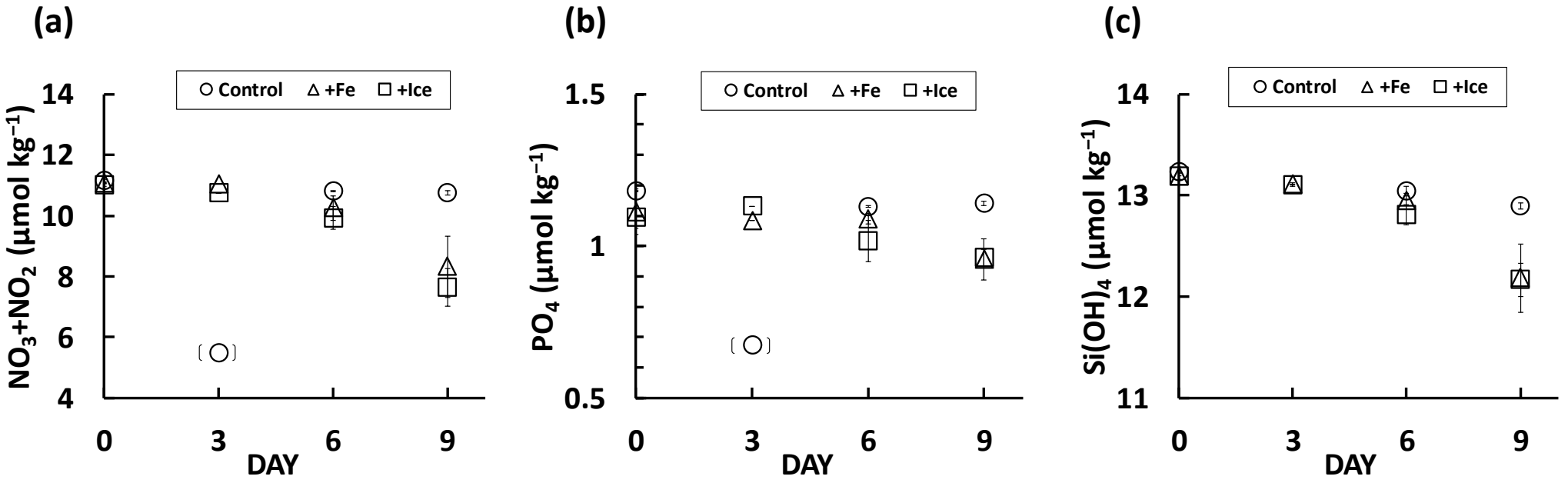
(a)
Control
+Fe
+Ice
NO_3+NO_2 (µmol kg^{-1})
14
12
10
8
6
4
0
3
6
9
DAY
(b)
Control
+Fe
+Ice
PO_4 (µmol kg^{-1})
1.5
1
0.5
0
3
6
9
DAY
(c)
Control
+Fe
+Ice
$Si(OH)_4$ (µmol kg^{-1})
14
13
12
11
0
3
6
9
DAY

Figure 6

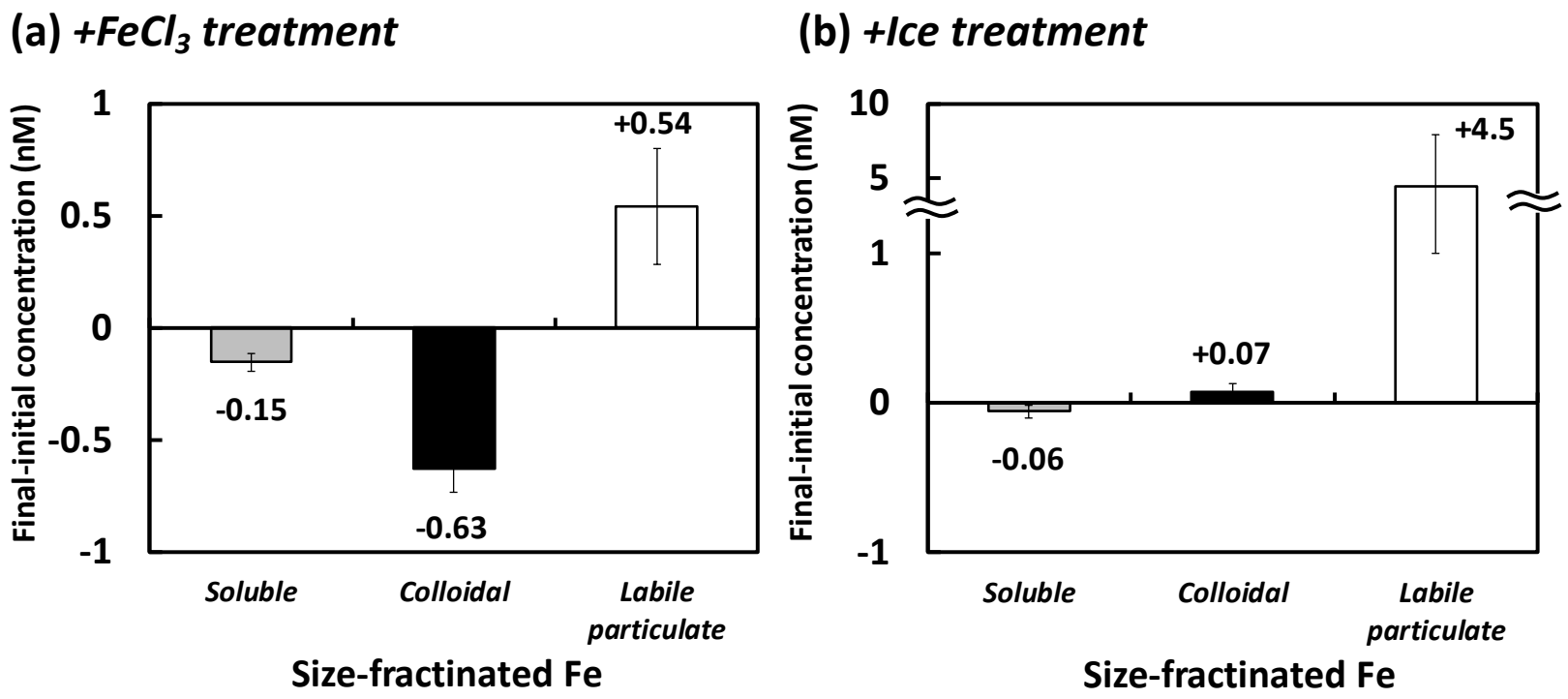
(a) +FeCl3 treatment
Final-initial concentration (nM)
1
0.5
0
-0.5
-1
-0.15
-0.63
+0.54
Soluble
Colloidal
Labile particulate
Size-fractinated Fe
(b) +Ice treatment
Final-initial concentration (nM)
10
5
1
0
-1
-0.06
+0.07
+4.5
Soluble
Colloidal
Labile particulate
Size-fractinated Fe

Figure 7

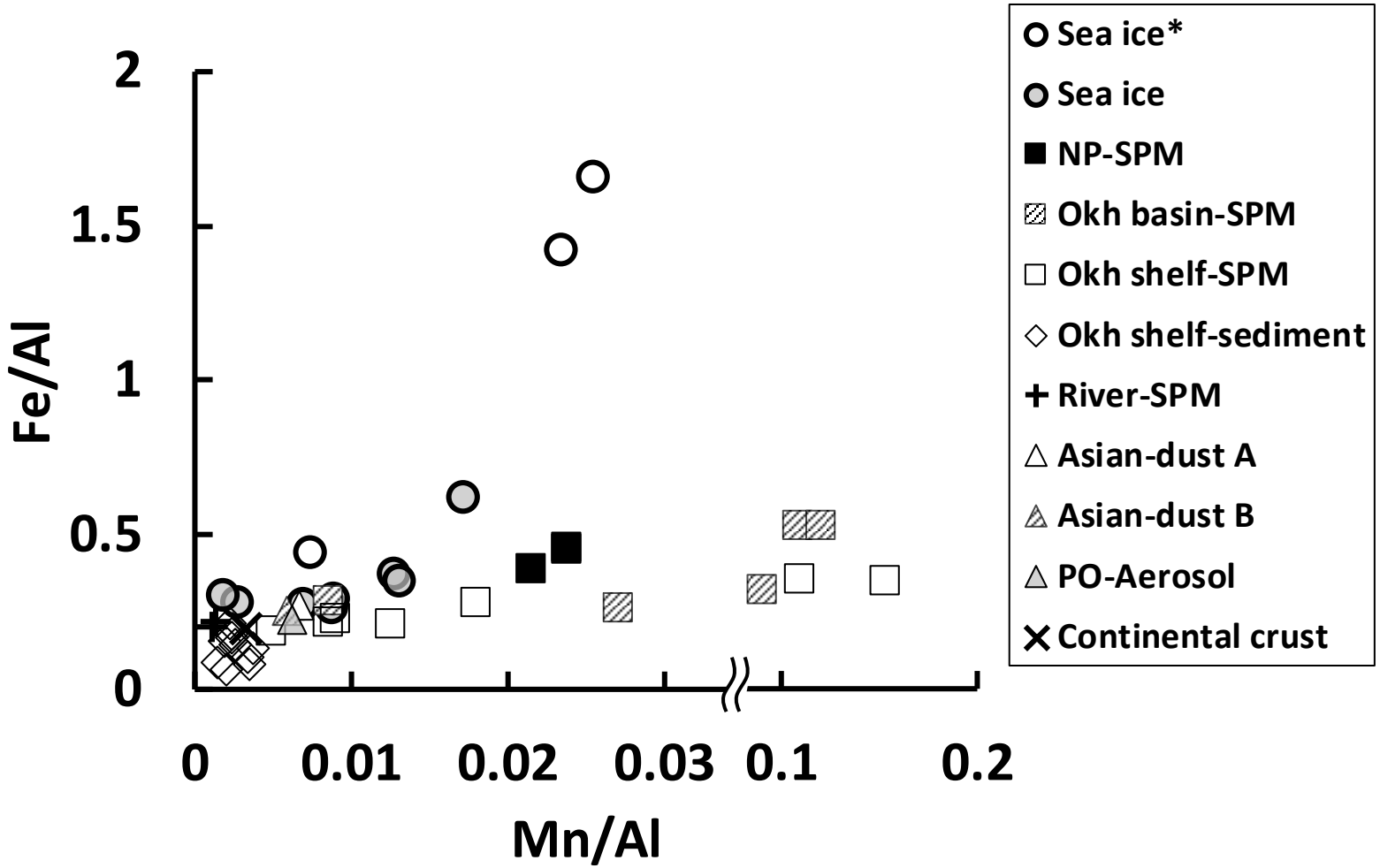
Fe/Al
2
1.5
1
0.5
0
0
0.01
0.02
0.03
0.1
0.2
Mn/Al
Sea ice*
Sea ice
NP-SPM
Okh basin-SPM
Okh shelf-SPM
Okh shelf-sediment
River-SPM
Asian-dust A
Asian-dust B
PO-Aerosol
Continental crust